Dalton Transactions

PAPER

FLP-type alkenylation of a phosphafluorene

Ayu Afiqah Nasrullah,[a,b] Tobias Täufer, [iD] [a] Jola Pospech, [iD] [a] Eszter Baráth [iD] *[a] and Christian Hering-Junghans [iD] *[a]

Phosphafluorenes, in which the chemically vulnerable C-9 position of the fluorene core has been replaced with phosphorus, demonstrate enhanced stability compared to conventional fluorene-based materials and belong to the general class of dibenzophospholes (DBPs). Phosphafluorene formation is commonly observed in the reductive functionalization of terphenyl-based dihalophosphanes. Here, we outline a high-yielding route towards phosphafluorene **1**, starting from readily available ^{Dipp}TerPCl$_2$ (^{Dipp}Ter = 2,6-Dipp-C$_6$H$_3$; Dipp = 2,6-iPr$_2$-C$_6$H$_3$). Different functionalization strategies of **1** are outlined, including a complex with AuCl, its BH$_3$ adduct, and its corresponding sulphide. Interestingly, facile alkenylation of **1** was achieved in the presence of B(C$_6$F$_5$)$_3$ and various phenylacetylene derivatives. This FLP-type alkenylation is *E*-selective giving zwitterionic phosphonium borates.

Introduction

Phosphanylidenephosphoranes of the general form RP(PR'$_3$) are also referred to as phospha-Wittig reagents.[1] Specifically, aryl-substituted variants are commonly used in phosphaalkene synthesis in the so-called phospha-Wittig reaction. The first aryl-substituted phosphanylidenephosphoranes, ArP(PMe$_3$), were synthesized by Protasiewicz and co-workers in 1998 through the combination of Ar–PCl$_2$ with an excess of PMe$_3$ and zinc powder.[2] To date a limited number of ArP(PMe$_3$) (Ar = 2,4,6-tBu$_3$–C$_6$H$_2$, Mes*;[2] 2,6-(2,6-Cl$_2$C$_6$H$_3$)$_2$–C$_6$H$_3$, ^{Cl}Ter;[3] 2,6-(2,4,6-Me$_3$–C$_6$H$_2$)$_2$–C$_6$H$_3$, ^{Mes}Ter;[2,4] 2,6-(2,4,6-iPr$_3$–C$_6$H$_2$)$_2$–C$_6$H$_3$, ^{Tipp}Ter;[5] 2,6-(2,6-iPr$_2$–C$_6$H$_3$)$_2$–C$_6$H$_3$, ^{Dipp}Ter;[6] 1,1,3,3,5,5,7,7-octaethyl-1,2,3,5,6,7-hexahydro-*s*-indacen-4-yl, EIND[7]) have been reported and their utility in Wittig-type reactions has been explored. Moreover, it was shown that phospha-Wittig reagents offer a pathway for the generation of arylphosphinidenes, Ar–P, under photochemical conditions. For example, when ^{Tipp}TerP(PMe$_3$) was irradiated at 365 nm the formation of a phosphafluorene was described, through insertion of the phosphinidene into one of the C$_{Ar}$–C$_{iPr}$ bonds of the Tipp groups.[5] Our group observed ^{Dipp}Ter–P generation and de-activation to give phosphafluorene **1** *via* the thermal decomposition of the isolated phosphagallene, ^{Dipp}TerPGaCp* at 50 °C for 2 h (Scheme 1a), or through the irradiation (396 nm) of

Scheme 1 (a) Thermal phosphinidene release from a phosphagallene; (b) photochemical PMe$_3$ release from ^{Dipp}TerP(PMe$_3$); (c and d) Lewis acid induced phosphafluorene formation in terphenyl-substituted halophosphanes; (e and f) reductive approaches towards phosphafluorenes from dichlorophosphanes (e and f); and summary of this work.

^{a}*Leibniz Institut für Katalyse e.V. (LIKAT), A.-Einstein-Str. 29a, 18059 Rostock, Germany. E-mail: eszter.barath@catalysis.de, Christian.hering-junghans@catalysis.de*

^{b}*Pusat Persediaan Sains dan Teknologi, Universiti Malaysia Sabah, Jln UMS, 88400 Kota Kinabalu, Sabah, Malaysia*

^{Dipp}TerP(PMe$_3$) in toluene-d_8 at room temperature (Scheme 1b).[8]

These findings complement earlier work on phosphafluorene formation *via* the reduction of ^{Tipp}TerPCl$_2$ with magnesium (Scheme 1f).[9] It was later shown that the reducing agent plays an important role in the outcome of the reaction.[10] Related cyclizations of terphenyl-based dichlorophosphanes were also described by Marshall[11] in the reduction with potassium (Scheme 1e), and by Wehmschulte and co-workers in AlCl$_3$-mediated Friedel–Crafts type reactions (Scheme 1c).[12] Similar intramolecular cyclizations have also been described for terphenyl-substituted phosphenium cations, allowing the isolation of the 9-phospha fluorenium ions (Scheme 1d).[13]

Phosphafluorenes, in which the chemically vulnerable C-9 position of the fluorene is replaced with phosphorus, belong to the broader class of dibenzophospholes (DBPs),[14] which are a family of compounds that have garnered significant interest due to their unique electronic properties and potential applications in materials science and catalysis. DBPs are important building blocks for organic π-conjugated compounds, which have enormous potential as optoelectronic materials for example in light-emitting diodes (OLED), organic field-effect transistors, nonlinear optical devices, and organic solar cells.[15–18] In recent years, monodentate non-symmetrical dibenzophospholes have emerged as ligands in rhodium-catalyzed hydroformylations.[19] Phosphafluorenes, demonstrate enhanced stability compared to conventional fluorene-based materials. They are usually blue-light-emitting materials,[15] and the photophysical properties can be precisely tuned through functionalization, especially at the phosphorus atom. Examples of functionalization strategies on the P center of phosphafluorenes include adduct formation with BH$_3$,[20] oxidation,[21] sulfurization,[22,23] complexation with tungsten, gold,[22,24] iron or ruthenium,[12] and related transformation.

DBPs can also be viewed as sterically encumbered phosphines, rendering them suitable candidates for frustrated Lewis pair (FLP) applications when paired with sterically hindered Lewis acids. The functionalization of alkynes using FLPs has been intensively studied.[25] The outcome of the reactions greatly depends on the basicity of the phosphine used. In the case of P/B-FLPs two outcomes are possible: (a) phosphonium alkynyl-borates, through deprotonation of the alkyne, or (b) addition to the alkynes resulting in zwitterionic alkenyl phosphonium borates, when less basic phosphines were employed.[26–28]

In this contribution, we report on different functionalization products of phosphafluorene 1 using BH$_3$, S$_8$ or AuCl. Moreover, the reactivity of 1 towards terminal alkynes (4-R–C$_6$H$_4$–C≡C–H) in the presence of B(C$_6$F$_5$)$_3$ was investigated, proving an FLP-type alkenylation strategy for DBPs (Scheme 1, bottom).

Results and discussion
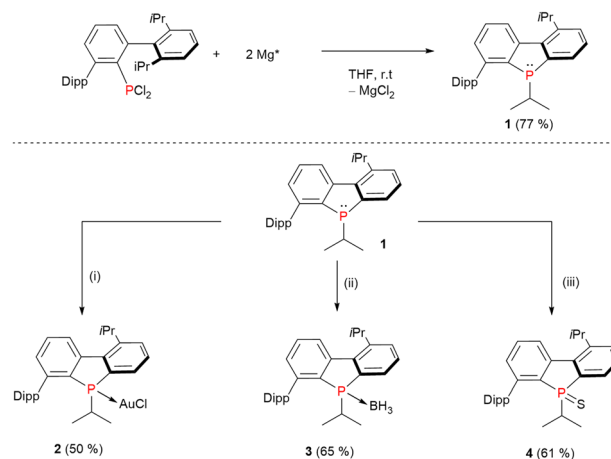
Rather than starting from ^{Dipp}TerP═GaCp* or ^{Dipp}TerP(PMe$_3$), phosphafluorene 1 is conveniently prepared through reduction

of ^{Dipp}TerPCl$_2$ with two equivalents of activated magnesium (Mg*, also see Scheme 1f).[9] After work-up, 1 was afforded as light orange, fluffy solid in 77% yield (Scheme 2, top). The formation of 1 was confirmed by ^{31}P NMR spectroscopy in C$_6$D$_6$ ($\delta(^{31}P\{^1H\})$ = −1.1 ppm) and a complex ^{1}H NMR spectrum, which shows a characteristic upfield-shifted pseudo-triplet ($\delta(^1H)$ = 0.26 ppm) for one of Me-groups of the P-iPr moiety, in line with C_1 symmetry in solution.

Next, chemical modifications at the P-center of 1, particularly through coordination to transition metals, sulfurization, and reactions with Lewis acids were targeted (Scheme 2, bottom). The combination of 1 with (Me$_2$S)AuCl in toluene afforded complex 2 (Scheme 2,i), which was recrystallized from a 1 : 5 CH$_2$Cl$_2$: n-hexane solution at −30 °C giving colourless single crystals suitable for single crystal X-ray diffraction (SCXRD) analysis and 2 was isolated in 50% yield. The ^{31}P$\{^1H\}$ NMR shift in C$_6$D$_6$ at 32.4 ppm indicated the formation of complex 2 and a tetracoordinate P atom. Upon coordination of AuCl, the $^3J_{P-H}$ coupling constant of the shielded Me-group ($\delta(^1H)$ = 0.04 ppm) increases and results in a clear doublet of doublet splitting of the signal. Phosphafluorene BH$_3$ adduct 3 (Scheme 2,ii) was obtained when stirring 1 and H$_3$B·SMe$_2$ in n-hexane. After crystallization from n-heptane at −30 °C 3 was isolated as colourless single crystalline material in 65% yield. The ^{31}P$\{^1H\}$ and ^{11}B $\{^1H\}$ NMR spectra of 3 in C$_6$D$_6$ displayed characteristic signals at 37.3 ppm and −38.4 ppm, respectively, indicating tetracoordinate P and B atoms. Additionally, the BH$_3$ moiety is detected in the IR spectrum, with B–H stretching modes centred at 2345 cm^{-1}.[29]

In the ^{1}H NMR spectrum, the expected quartet resonance for BH$_3$ is significantly broadened and overlaps with the signals of the iPr–Me groups and could therefore not be unambiguously assigned. Similarly to 2, the shielded Me-groups of the iPr-groups on the P atom changes into a doublet of doublets.

Scheme 2 Synthesis of phosphafluorene 1 (top). Functionalization of the phosphorus center in 1: (i) AuCl·SMe$_2$, toluene, 16 h, r.t.; (ii) H$_3$B·SMe$_2$, n-hexane, 16 h, r.t.; (iii) 1/8 S$_8$, CH$_2$Cl$_2$, 16 h, r.t.

The reaction of **1** with elemental sulfur cleanly furnished thiophosphafluorene **4** as a white solid in 61% isolated yield. The ^{31}P NMR signal of **4** ($\delta(^{31}P\{^{1}H\})$ = 53.4 ppm; $\Delta_{1-4}(\delta(^{31}P))$ = +54.5 ppm) is notably deshielded compared to **2** and **3**, consistent with P=S bond formation. A similar deshielding is observed in related dibenzophosphapentaphenes upon sulfurization (cf. $\Delta(\delta(^{31}P))$ = +48.9 ppm).[22] SCXRD experiments (Fig. 1) revealed that **2**, **4** and **3** crystallize in the monoclinic space groups $P2_1/c$ and $P2_1/n$, respectively. **2–4** show a four-coordinate P atom ($\sum(<P)$ = 304.1(1) (**2**), 307.01(6) (**3**), 303.0(6)° (**4**)). The P–C_{Ar} distances (**2**: 1.798(2), 1.805(2); **3**: 1.799(1), 1.810(1); **4**: 1.797(1), 1.809(1) Å) are shorter compared to the related free phosphafluorene derived from ^{TiPP}TerPCl$_2$ (cf. 1.805(11), 1.817 (4) Å).[9] Similarly, the P–C_{iPr} (**2**: 1.845(2); **3**: 1.844(1); **4**: 1.866(1) Å) bonds in **2** and **3** are contracted compared to the related phosphafluorene. The P1–Au1 bond distance (2.2247(6) Å) in **2** aligns with reported gold(I) P-heterocycle complexes,[24,30] the P–B distance in BH$_3$-adduct **3** (1.9269(16) Å) is in the range of reported dibenzophosphole BH$_3$ adducts,[31] and the P–S distance aligns with that in dibenzophosphapentaphene sulfides.[22]

In an effort to identify alternative Lewis acids to H$_3$B·SMe$_3$, we explored bulkier derivatives such as B(C$_6$F$_5$)$_3$. When **1** and B(C$_6$F$_5$)$_3$ were combined in a 1 : 1 ratio in C$_6$D$_6$, no discernible reaction was observed according to ^{31}P NMR spectroscopy. This lack of reactivity suggests frustrated Lewis pair (FLP) behaviour arising from steric congestion between the Lewis acid and base. Upon addition of one equivalent phenylacetylene to the reaction mixture in C$_6$D$_6$, the color of the solution changes from light orange to dark red. NMR data of the reaction mixture showed complete conversion to a new species. Layering of the reaction mixture in C$_6$D$_6$ with n-hexane at ambient temperature and standing overnight afforded a white powder of [P]C(Ph)=C(H)B(C$_6$F$_5$)$_3$ (**5**; [P] = 1-

(2,6-diisopropylphenyl)-5,9-diisopropyl-9-phosphafluorene) and was isolated in 61% yield. Compound **5** features a ^{1}H NMR resonance at 7.84 ppm (d, $^{3}J_{P-H}$ = 38.0 Hz) assigned to the alkenyl C=CH moiety (cf. Ph$_3$P(PhC=CH)B(C$_6$F$_5$)$_3$: $\delta(^{1}H)$ = 8.32 ppm, $^{3}J_{P-H}$ = 36.0 Hz).[26] The ^{31}P NMR signal at 36.1 ppm is in line with a phosphonium center, whereas the ^{19}F NMR spectrum showed three sets of signals for the o-, p-, and m-fluorine atoms of the C$_6$F$_5$ groups located at $\delta(^{19}F)$ −130.5, −161.7, and −166 ppm, respectively, in line with reported FLP-type activations of phenylacetylene and free rotation about the B–C axis.[26] In the ^{11}B NMR spectrum, a signal at −15.4 ppm (d, $^{3}J_{P-H}$ = 18.0 Hz) is in line with a four-coordinate boron center and a zwitterionic phosphonium borate species. Collectively these data suggested that **5** is exclusively the 1,2-addition product (Scheme 3, bottom). This assumption was confirmed by X-ray crystallography showing that the phosphine and borane added to the alkyne in (E)-fashion with the B adding to the CH terminus of the alkyne (Fig. 2, left).[27] The solid-state structure reveals P–C_{Ar} (1.792 (2), 1.801(2) Å) and P–C_{iPr} (1.828(2) Å) distances similar to those found in **2** and **3** (vide supra). The P–$C_{C=C}$ distance (1.828(2) Å) is in the range of a contracted P–C single bond ($\sum r_{cov}$(P–C) = 1.86 Å)[32] and minimally longer than in Ph$_3$P (PhC=CH)B(C$_6$F$_5$)$_3$ (cf. 1.806(1) Å).[26] The C31–C32 distance (1.344(2), cf. $\sum r_{cov}$(C=C) = 1.34 Å)[32] clearly indicates activation of the alkyne unit, with the P and B atoms being in $trans$-orientation with respect to the C=C bond. Notably, the
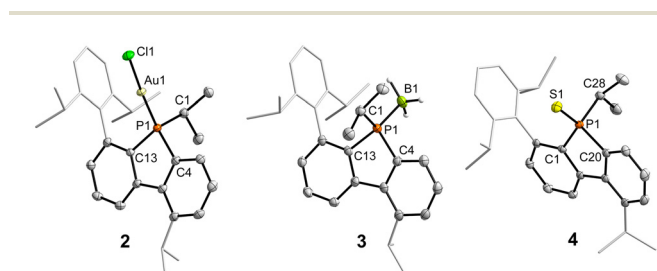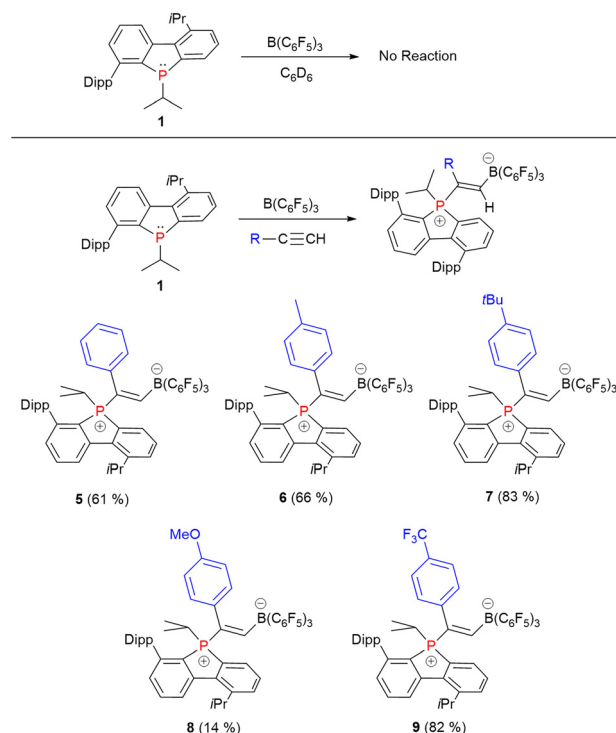

Fig. 1 Molecular structures of **2** (left), **3** (middle) and **4** (right). Ellipsoids drawn at 50% with C–H-atoms omitted, Dipp- and one of the iPr-groups rendered as wire-frame for clarity. Selected bond lengths [Å] and angles [°] of **2**: C1–P1 1.845(2), C4–P1 1.798(2), C13–P1 1.805(2), P1–Au1 2.2247(6), Cl1–Au1 2.2885(6); C4–P1–C13 91.83(10), C4–P1–C1 106.46 (10), C13–P1–C1 105.84(10), C4–P1–Au1 114.61(7), C13–P1–Au1 121.62 (7), C1–P1–Au1 113.71(8); C5–C4–P1–C13 179.9(2). **3**: P1–C4 1.7991(13), P1–C13 1.8102(13), P1–C1 1.8435(14), P1–B1 1.9269(16); C4–P1–C13 91.52(6), C4–P1–C1 108.29(6), C13–P1–C1 107.20(6), C4–P1–B1 111.38 (7), C13–P1–B1 121.08(6), C1–P1–B1 114.62(7); C13–P1–C4–C9 −178.84 (12); **4**: P1–C1 1.809(1), P1–C20 1.797(1), P1–C28 1.866(1), P1–S1 1.9462 (5); C20–P1–C1 91.78(6), C20–P1–C28 106.39(6), C1–P1–C28 104.83 (6), C28–P1–S1 112.84(5); C20–P1–C1–C2 175.58(12).

Scheme 3 Reactivity of **1** towards B(C$_6$F$_5$)$_3$ in the absence (top) and presence of phenylacetylene derivatives, giving alkenyl phosphonium borates **5–9**.
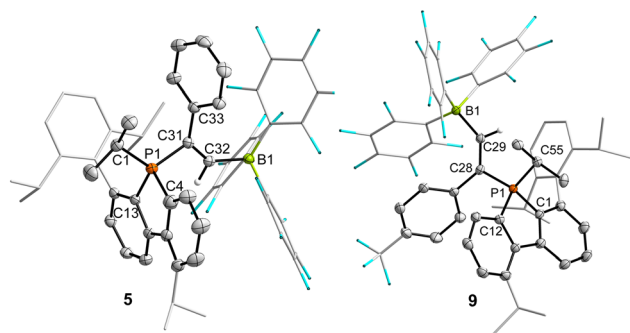
Fig. 2 Molecular structures of **5** and **9**. Ellipsoids drawn at 50% with C–H-atoms omitted (except those at C32 (**5**) and C29(**9**)), Dipp-, C_6F_5-, CF_3- and one of the iPr-groups rendered as wire-frame for clarity. Selected bond lengths [Å] and angles [°] of **5**: P1–C4 1.7915(18), P1–C13 1.8014(16), P1–C1 1.8282(18), P1–C31 1.8282(17), B1–C32 1.648(2), C31–C32 1.344(2); C4 P1 C13 93.34(8), C4–P1–C1 110.49(8), C13–P1–C1 113.17(8), C4–P1–C31 107.19(8), C13–P1–C31 112.12(7), C1–P1–C31 117.64(8), C32–C31–P1 112.79(12), C31–C32–B1 138.96(15); C4–P1–C31–C32 65.08(14). **9**: C1–P1 1.8007(14), C12–P1 1.7807(14), C28–P1 1.7969(13), C55–P1 1.8326(14), C28–C29 1.3433(19), C29–B1 1.642(2); C12–P1–C28 108.96(6), C12–P1–C1 93.52(6), C28–P1–C1 122.55(6), C12–P1–C55 108.64(7), C28–P1–C55 113.19(6), C1–P1–C55 107.71(6), C29–C28–P1 116.86(10), C28–C29–B1 136.79(13); C29–C28–P1–C12 137.25(11).

C≡C*H* proton is oriented towards the phosphafluorene moiety.

Motivated by these findings, we next tested a series of *para*-substituted phenylacetylenes (4-R–C_6H_4–C≡CH where R = CH_3 (**6**), *t*Bu (**7**), OMe (**8**), CF_3 (**9**)) to investigate possible substituent effects on this FLP reactivity. Reaction of these alkynes with the **1**/B(C_6F_5)₃ FLP system proceeded analogously to **5**, yielding diverse zwitterionic alkenyl phosphonium borate products (Scheme 3), which underlines the generality of this functionalization strategy.[27] This FLP-type alkenylation of a P-heterocycle is also related to the chemistry of phosphinine-borane adducts towards phenylacetylene.[33] The ³¹P NMR shifts for **6–9** are clustered near 36.0 ppm, clearly showing minimal influence of the *para*-substituent. All compounds (**6–9**) displayed ¹⁹F NMR signals for the B(C_6F_5)₃ moiety in the range of −130.5 (*ortho*-F), −161.7 (*para*-F), and −166.0 (*meta*-F), mirroring **5**, and thereby indicating a similar B(C_6F_5)₃ moiety in all alkenylation products **5–9**. Notably, **9** showed an additional singlet at −63.3 ppm in the ¹⁹F NMR spectrum assigned to the CF_3 group. The ¹¹B NMR spectra of **6–9** uniformly exhibited resonances near −15.0 ppm (d, ³J_{P-B} = 18 Hz) as expected for borate-type activation products. These observations suggest minimal electronic influence from the *para*-substituents of phenylacetylenes (EDG/EWG) on the regio- and chemoselectively of the alkenylation. In all derivatives the C≡CH resonance is deshielded at *ca.* 8 ppm and a ³J_{P-H} coupling constant of *ca.* 38 Hz.

These results underscore the robustness of FLP-mediated alkyne activation, where steric and electronic perturbations at the *para*-position are effectively reduced by the conjugated aromatic system, preserving the core electronic structure of the adducts.

Single crystals of **9** suitable for SCXRD were obtained from layering the C_6D_6 reaction mixture with *n*-heptane at room temperature. As previously observed in **5**, the alkyne activation is (*E*)-selective, with boron attached to the CH terminus (Fig. 2, right). All key structural parameters are similar to those found in **5**. However, the orientation of the C≡C*H* proton is different, which is now oriented towards the P–iPr group.

Lastly, the absorption and emission profiles of **1** and its derivatives in MeCN solution were investigated. Phosphafluorene **1** shows absorption maxima in the UVB region at 303 and 312 nm and weak blue fluorescence with a broad emission maximum at 369 nm. As a representative for P-functionalized species **2–4**, phosphafluorene **4** was studied and shows two bathochromically shifted absorption maxima at 313 and 323 nm, while the emission maximum is hypsochromically shifted to 361 nm (Fig. 3). A second emission maximum is evident at 453 nm. Notably, the emission band is rather broad and tails into the visible region, in line with blue fluorescence in MeCN solution. Interestingly, the absorption spectra of alkenylated species **5–9** are nearly identical with absorption maxima at *ca.* 330 nm (Fig. 4), indicating minimal influence of the *para*-substituent in the employed phenyl-acetylene derivatives. The emission spectrum of **5** features a maximum at 381 nm with a shoulder at 400 nm (Fig. S66). Broad emission maxima between 380–390 nm are detected for **6**, **7** and **9**. Compound **8** displays distinct photophysical characteristics, featuring a minor absorption shoulder at 385 nm, while the emission maximum is markedly red-shifted to 472 nm. In the absence of lifetime data, we tentatively attribute this pronounced red-shift to phosphorescence rather than fluorescence or a chemical transformation in the excited state. Generally, P-functionalization in **4** results in a red-shift of the absorption maximum, which is even more pronounced
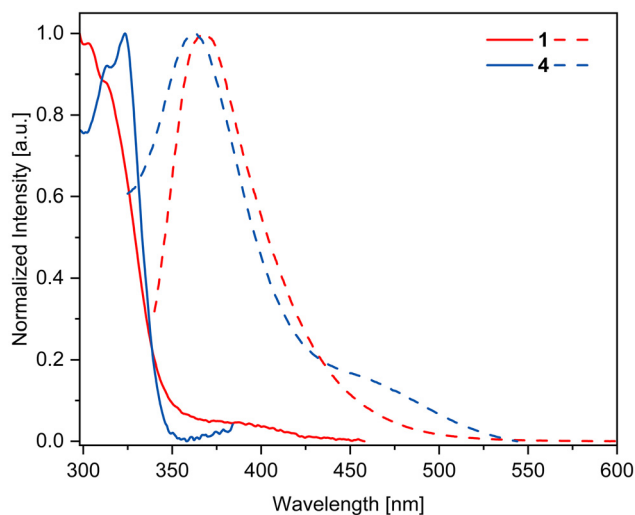

Fig. 3 Normalized absorption- (compact) and emission (dashed) spectra of **1** and **4**.
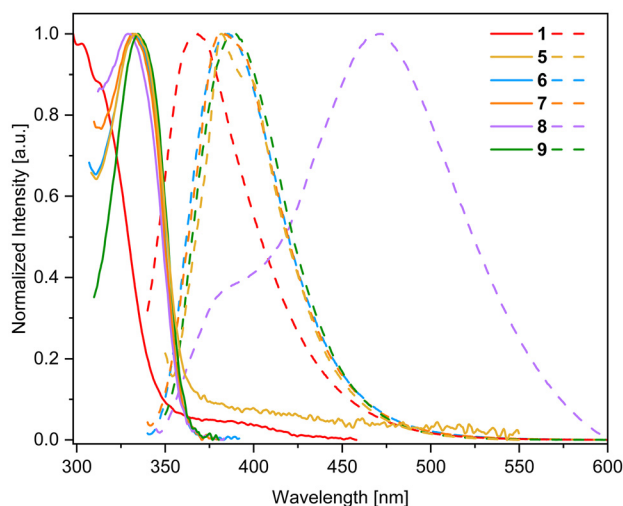
Fig. 4 Normalized absorption- (compact) and emission (dashed) spectra of **1** and **5–9**.

for the alkenylated species **5–9**. This agrees with previous studies that have clearly shown that P-functionalization will result in bathochromically shifted absorption bands.[15,22] The absorption and emission spectra of **4** and **8** show no mirror relation, indicating significant structural rearrangements in the exited state. Consistent with previous reports, the Stokes shift in phosphafluorene luminescence is rather large.

Conclusions

We outline a facile synthetic route towards phosphafluorene **1** starting from readily accessible ^{DiPP}TerPCl$_2$ in a reductive approach. Quarternization of **1** with AuCl, BH$_3$, and sulphur afforded P-functionalized species **2–4**, respectively. When **1** was combined with B(C$_6$F$_5$)$_3$ no reaction was observed. Adding phenylacetylene to the mixture, clean FLP-type alkenylation of the P atom in **1** was noted giving (*E*)-configured alkenyl phosphonium borate **5**. This novel alkenylation strategy for DBPs was extended and facile conversion with *para*-substituted phenylacetylenes was achieved giving species **6–9**. To the best of our knowledge this is the first report on FLP-type functionalization of DBPs and the generality of the concept with respect to the DBP-precursors is currently investigated. It needs to be stated that all compounds in this paper are P-chiral and paths to render these transformations enantioselective will be studied in the future. Furthermore, the photophysical properties of the alkenylation products will be studied in more detail.

Author contributions

A. A. N. carried out the experimental work, wrote the SI and drafted the manuscript. C. H.-J. was responsible for the conceptualization, supervision of the experimental investigations,

solved and refined the SCXRD structures. T. T. and J. P. carried out the photophysical characterization. J. P., C. H.-J. and E. B. finalized the manuscript. All authors agreed to the submitted content.

Conflicts of interest

There are no conflicts to declare.

Data availability

The data supporting this article have been included as part of the SI: synthesis and characterization of compounds, NMR spectra, additional spectroscopic data and crystallographic details. See DOI: **https://doi.org/10.1039/d5dt01495f**.

CCDC 2466772 (**2**), 2466773 (**3**), 2482916 (**4**), 2466774 (**5**) and 2466775 (**9**) contain the supplementary crystallographic data for this paper.[34a–e]

Acknowledgements

References

1 J. D. Protasiewicz, *Eur. J. Inorg. Chem.*, 2012, **2012**, 4539–4549.

2 S. Shah and J. D. Protasiewicz, *Chem. Commun.*, 1998, 1585–1586.

3 R. C. Smith, T. Ren and J. D. Protasiewicz, *Eur. J. Inorg. Chem.*, 2002, **2002**, 2779–2783.

4 S. Shah, G. P. A. Yap and J. D. Protasiewicz, *J. Organomet. Chem.*, 2000, **608**, 12–20.

5 S. Shah, M. C. Simpson, R. C. Smith and J. D. Protasiewicz, *J. Am. Chem. Soc.*, 2001, **123**, 6925–6926.

6 P. Gupta, J.-E. Siewert, T. Wellnitz, M. Fischer, W. Baumann, T. Beweries and C. Hering-Junghans, *Dalton Trans.*, 2021, **50**, 1838–1844.

7 K. Takeuchi, H.-O. Taguchi, I. Tanigawa, S. Tsujimoto, T. Matsuo, H. Tanaka, K. Yoshizawa and F. Ozawa, *Angew. Chem., Int. Ed.*, 2016, **55**, 15347–15350.

8 T. Taeufer, F. Dankert, D. Michalik, J. Pospech, J. Bresien and C. Hering-Junghans, *Chem. Sci.*, 2023, **14**, 3018–3023.

9 B. Twamley, C. D. Sofield, M. M. Olmstead and P. P. Power, *J. Am. Chem. Soc.*, 1999, **121**, 3357–3367.

10 R. C. Smith, S. Shah and J. D. Protasiewicz, *J. Organomet. Chem.*, 2002, **646**, 255–261.

11 A. S. Ionkin and W. J. Marshall, *Heteroat. Chem.*, 2003, **14**, 360–364.

12 A. A. Diaz, J. D. Young, M. A. Khan and R. J. Wehmschulte, *Inorg. Chem.*, 2006, **45**, 5568–5575.

13 M. Olaru, D. Duvinage, Y. Naß, L. A. Malaspina, S. Mebs and J. Beckmann, *Angew. Chem., Int. Ed.*, 2020, **59**, 14414–14417.

14 P. Hibner-Kulicka, J. A. Joule, J. Skalik and P. Bałczewski, *RSC Adv.*, 2017, **7**, 9194–9236.

15 J. Yin, R.-F. Chen, S.-L. Zhang, Q.-D. Ling and W. Huang, *J. Phys. Chem. A*, 2010, **114**, 3655–3667.

16 H.-C. Su, O. Fadhel, C.-J. Yang, T.-Y. Cho, C. Fave, M. Hissler, C.-C. Wu and R. Réau, *J. Am. Chem. Soc.*, 2006, **128**, 983–995.

17 C.-H. Lin, C.-W. Hsu, J.-L. Liao, Y.-M. Cheng, Y. Chi, T.-Y. Lin, M.-W. Chung, P.-T. Chou, G.-H. Lee, C.-H. Chang, C.-Y. Shih and C.-L. Ho, *J. Mater. Chem.*, 2012, **22**, 10684–10694.

18 X. Deng, S. Liu, Y. Sun, D. Zhong, D. Jia, X. Yang, B. Su, Y. Sun, G. Zhou, B. Jiao and Z. Wu, *Dyes Pigm.*, 2023, **209**, 110885.

19 A. Oukhrib, L. Bonnafoux, A. Panossian, S. Waifang, D. H. Nguyen, M. Urrutigoity, F. Colobert, M. Gouygou and F. R. Leroux, *Tetrahedron*, 2014, **70**, 1431–1436.

20 K. V. Rajendran and D. G. Gilheany, *Chem. Commun.*, 2012, **48**, 817–819.

21 H. A. van Kalkeren, S. H. A. M. Leenders, C. R. A. Hommersom, F. P. J. T. Rutjes and F. L. van Delft, *Chem. – Eur. J.*, 2011, **17**, 11290–11295.

22 P.-A. Bouit, A. Escande, R. Szűcs, D. Szieberth, C. Lescop, L. Nyulászi, M. Hissler and R. Réau, *J. Am. Chem. Soc.*, 2012, **134**, 6524–6527.

23 J. A. Macor, J. L. Brown, J. N. Cross, S. R. Daly, A. J. Gaunt, G. S. Girolami, M. T. Janicke, S. A. Kozimor, M. P. Neu, A. C. Olson, S. D. Reilly and B. L. Scott, *Dalton Trans.*, 2015, **44**, 18923–18936.

24 R. Inaba, K. Oka, T. Iwami, Y. Miyake, K. Tajima, H. Imoto and K. Naka, *Inorg. Chem.*, 2022, **61**, 7318–7326.

25 J. Guo, M. Yan and D. W. Stephan, *Org. Chem. Front.*, 2024, **11**, 2375–2396.

26 M. A. Dureen and D. W. Stephan, *J. Am. Chem. Soc.*, 2009, **131**, 8396–8397.

27 M. A. Dureen, C. C. Brown and D. W. Stephan, *Organometallics*, 2010, **29**, 6594–6607.

28 C. Jiang, O. Blacque and H. Berke, *Organometallics*, 2010, **29**, 125–133.

29 C. A. Jaska, H. Dorn, A. J. Lough and I. Manners, *Chem. – Eur. J.*, 2003, **9**, 271–281.

30 S. Attar, W. H. Bearden, N. W. Alcock, E. C. Alyea and J. H. Nelson, *Inorg. Chem.*, 1990, **29**, 425–433.

31 V. Diemer, A. Berthelot, J. Bayardon, S. Jugé, F. R. Leroux and F. Colobert, *J. Org. Chem.*, 2012, **77**, 6117–6127.

32 P. Pyykkö and M. Atsumi, *Chem. – Eur. J.*, 2009, **15**, 12770–12779.

33 J. Lin, F. Wossidlo, N. T. Coles, M. Weber, S. Steinhauer, T. Böttcher and C. Müller, *Chem. – Eur. J.*, 2022, **28**, e202104135.

34 (*a*) A.A. Nasrullah, T. Täufer, J. Pospech, E. Baráth and C. Hering-Junghans, CCDC 2466772: Experimental Crystal Structure Determination, 2025, DOI: **10.5517/ccdc.csd.cc2nsw9n**; (*b*) A.A. Nasrullah, T. Täufer, J. Pospech, E. Baráth and C. Hering-Junghans, CCDC 2466773: Experimental Crystal Structure Determination, 2025, DOI: **10.5517/ccdc.csd.cc2nswbp**; (*c*) A.A. Nasrullah, T. Täufer, J. Pospech, E. Baráth and C. Hering-Junghans, CCDC 2482916: Experimental Crystal Structure Determination, 2025, DOI: **10.5517/ccdc.csd.cc2pbp2t**; (*d*) A.A. Nasrullah, T. Täufer, J. Pospech, E. Baráth and C. Hering-Junghans, CCDC 2466774: Experimental Crystal Structure Determination, 2025, DOI: **10.5517/ccdc.csd.cc2nswcq**; (*e*) A.A. Nasrullah, T. Täufer, J. Pospech, E. Baráth and C. Hering-Junghans, CCDC 2466775: Experimental Crystal Structure Determination, 2025, DOI: **10.5517/ccdc.csd.cc2nswdr**.